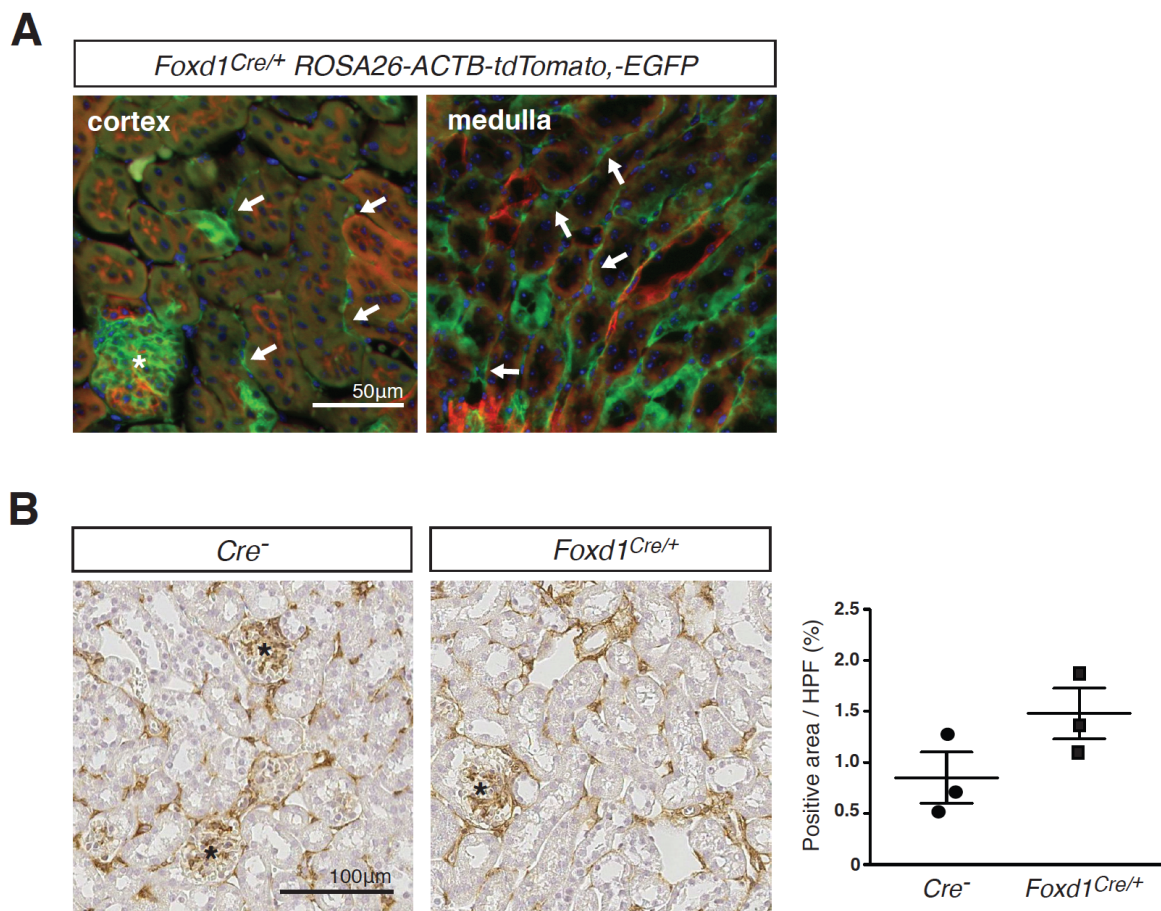
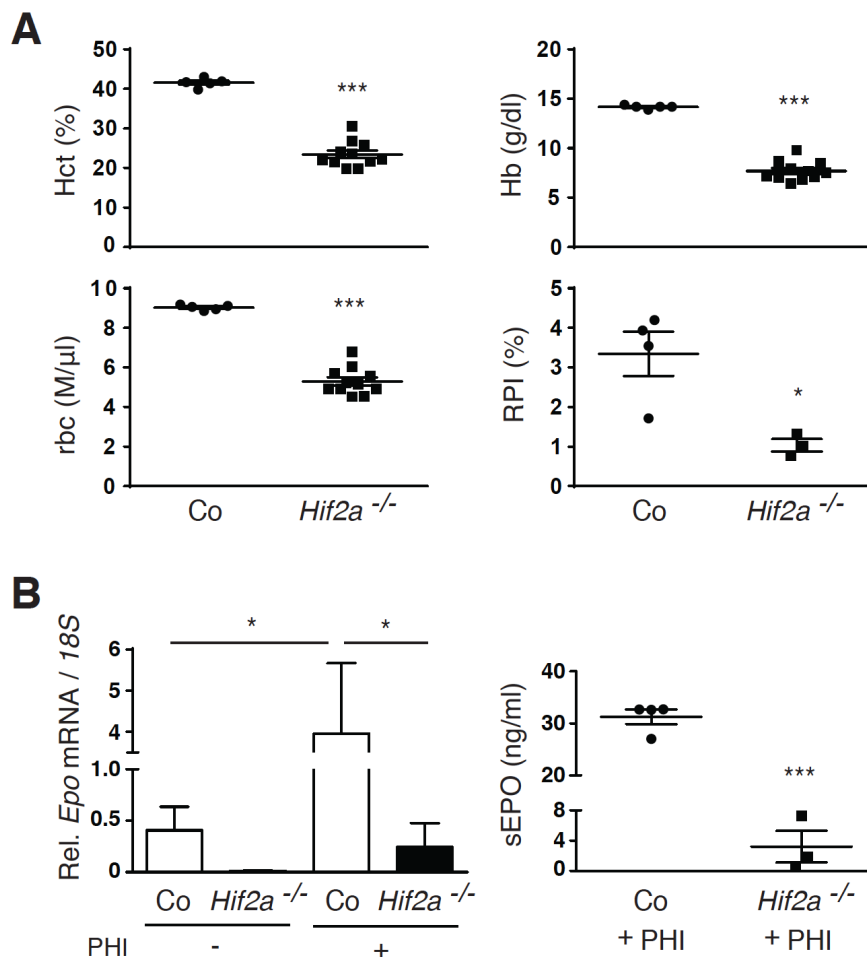


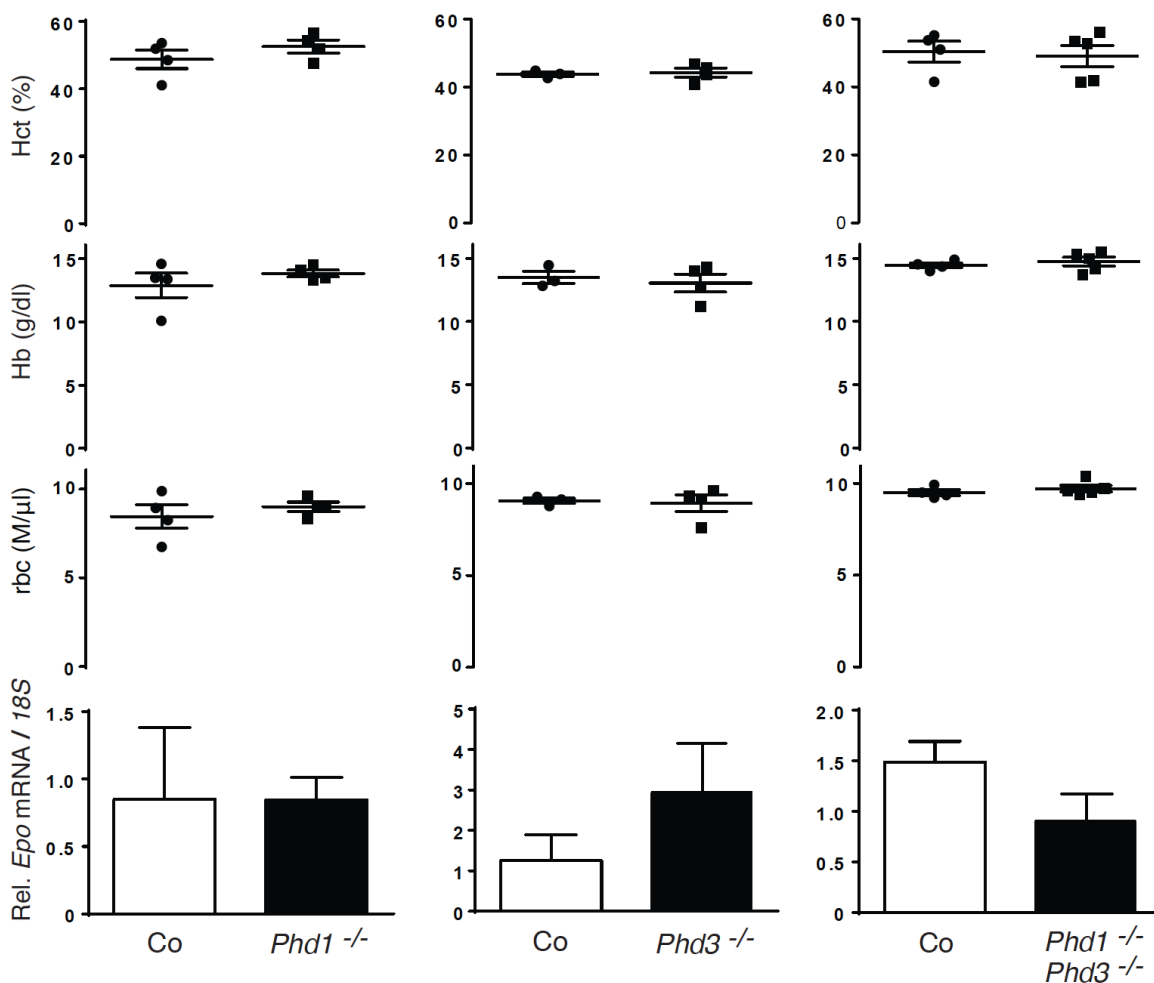
SUPPLEMENTAL MATERIAL



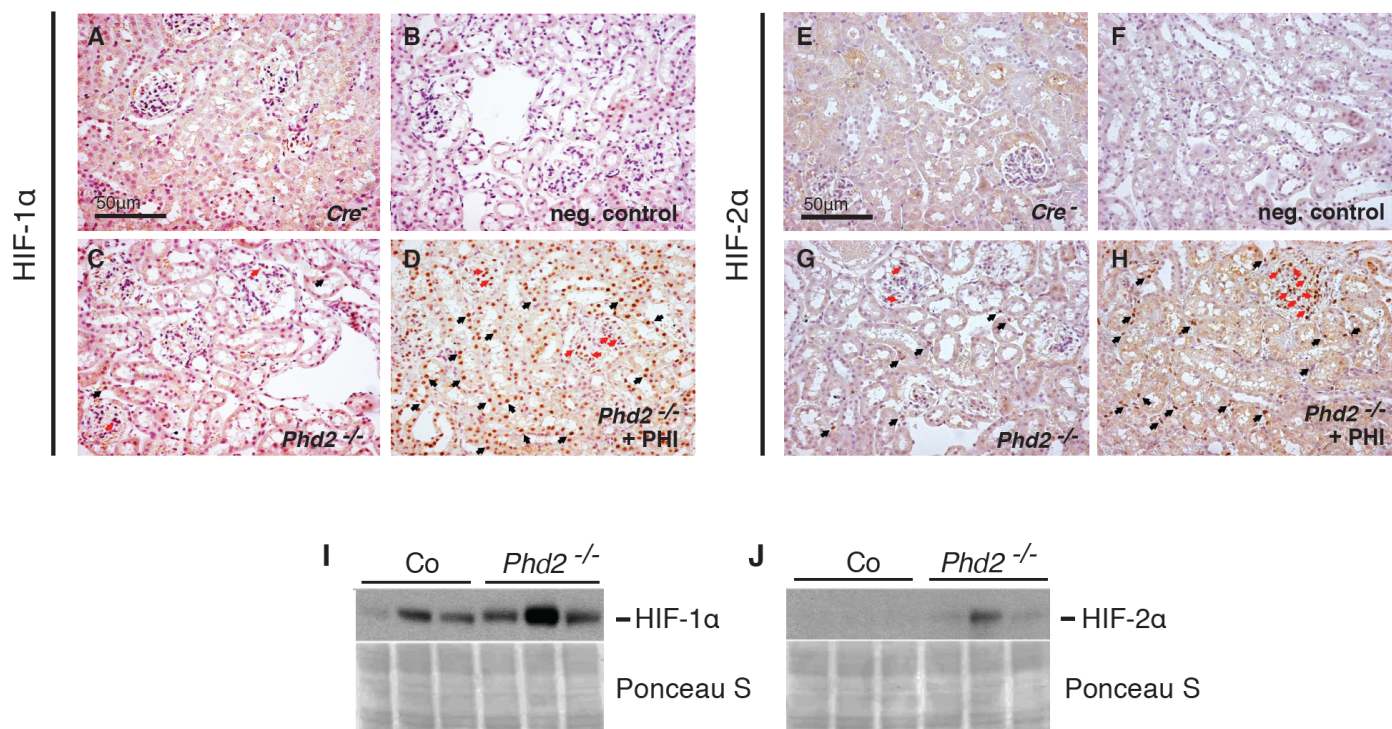
Supplemental Figure 1. *Foxd1*-Cre-mediated recombination in the kidney. (A) Representative images of renal cortex and medulla. Kidney sections were obtained from *Foxd1^{Cre/+} ROSA26-ACTB-tdTomato,-EGFP* mice and analyzed by fluorescence microscopy. *Foxd1*-Cre targeted cells express EGFP (green fluorescence), non-recombined cells express membrane-bound tdTomato red (red fluorescence). White arrows depict green fluorescent peritubular interstitial cells; asterisk depicts glomerulus. (B) Representative images of IHC for PDGFRB in formalin-fixed paraffin-embedded kidney tissue sections from *Cre⁻* and *Foxd1^{Cre/+} ROSA26-ACTB-tdTomato,-EGFP* (*Foxd1^{Cre/+}*) mice and quantification of PDGFRB-positive area per high power field (HPF). Data represent mean \pm SEM and were analyzed by 2-tailed Student's t-test. Significant differences were not found between groups. Asterisks depict glomeruli.



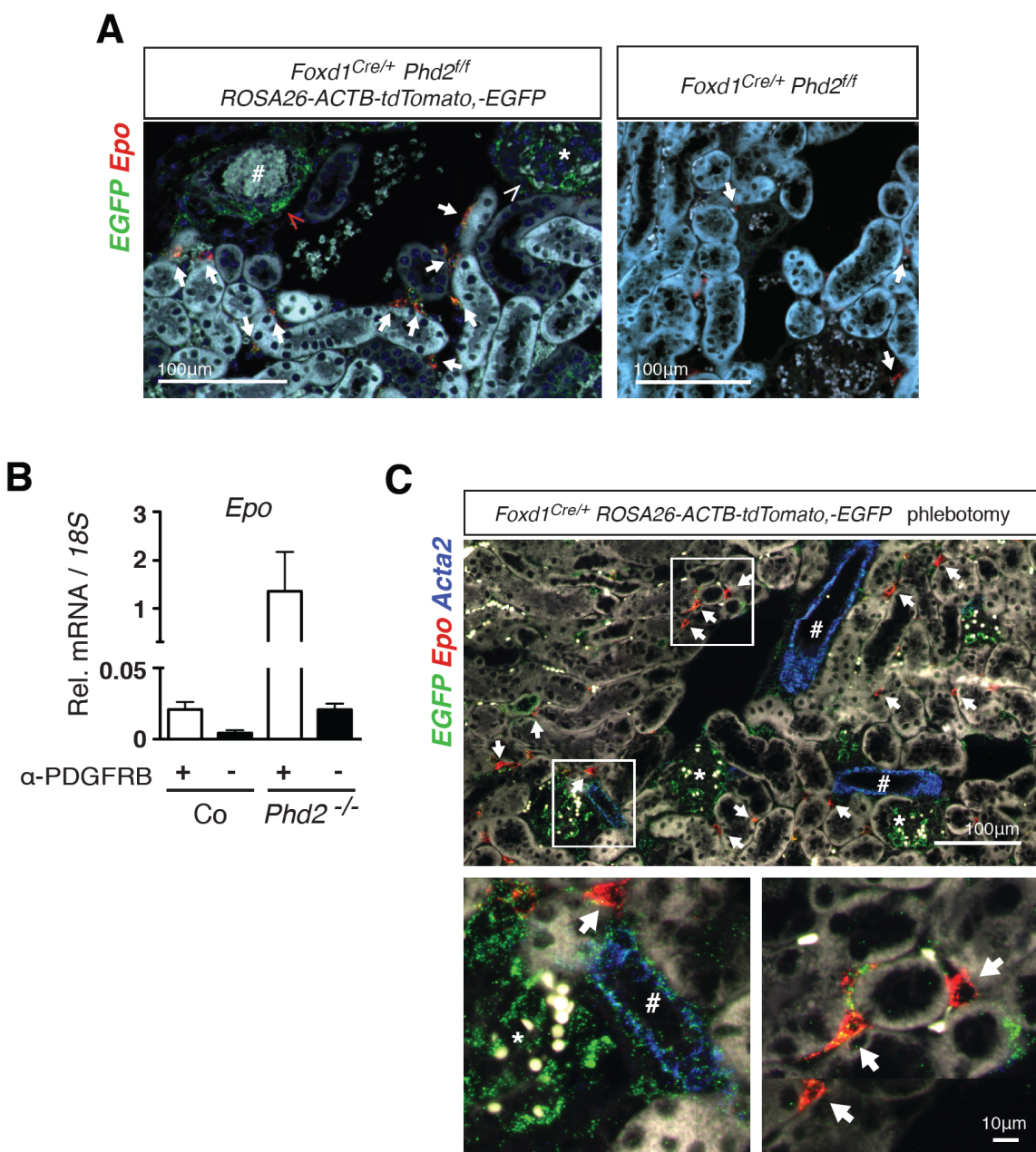
Supplemental Figure 2. Inactivation of *Hif2a* in FOXD1 stroma-derived interstitial cells results in anemia. (A) Shown are hematocrit, hemoglobin, rbc counts and reticulocyte production index (RPI) for individual *Cre*⁻ control (Co) and *Foxd1*^{Cre/+} *Hif2a*^{flox/flox} (*Hif2a*^{-/-}) mutant mice (n=5 and 11 respectively for Hct, Hb, and rbc; n=4 and 3 respectively for RPI). Data are represented as mean \pm SEM; 2-tailed Student's *t*-test; **P* < 0.05; ****P* < 0.001. (B) Renal *Epo* mRNA levels relative to 18S and serum EPO (sEPO) levels in *Cre*⁻ control (n=4) and *Foxd1*^{Cre/+} *Hif2a*^{flox/flox} mutant mice (n=3) treated with vehicle or with GSK1002083A (PHI). Data are represented as mean \pm SEM; 2-way ANOVA with post hoc Tukey's test for *Epo* mRNA panel; 2-tailed Student's *t*-test for sEPO panel; **P* < 0.05 and ****P* < 0.001 when compared to control.



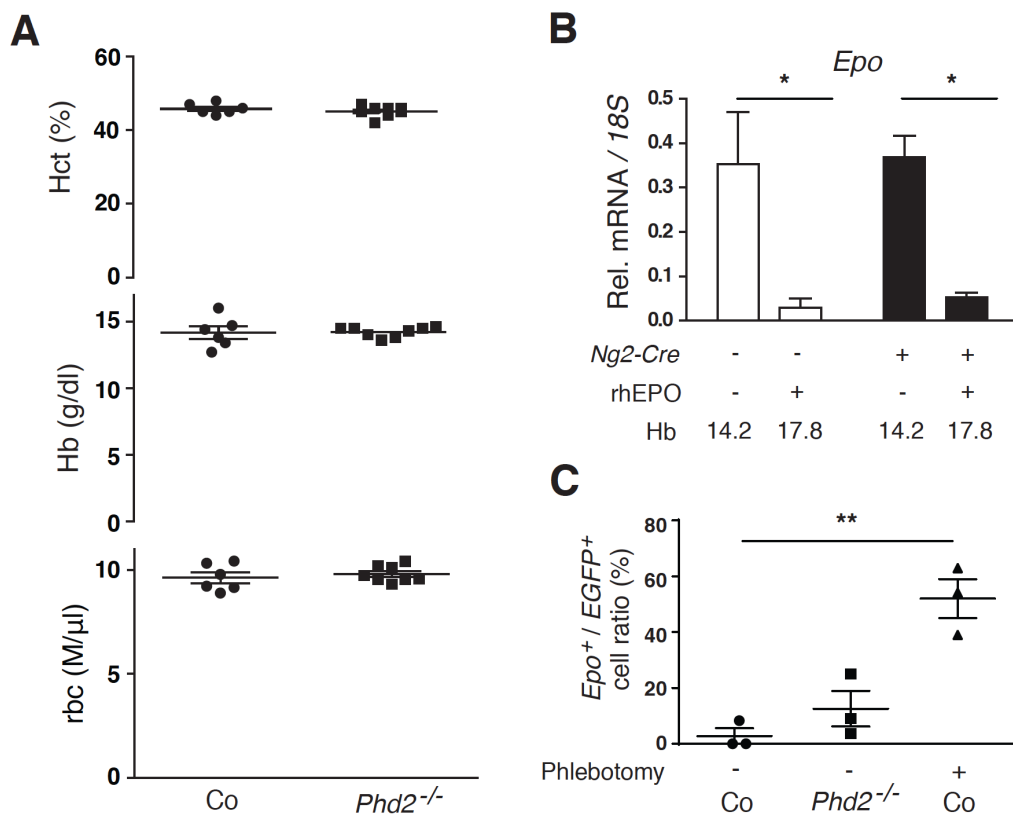
Supplemental Figure 3. Inactivation of *Phd1* and/or *Phd3* in FOXD1 stroma-derived interstitial cells does not affect renal *Epo* transcription. Shown are hematocrit, hemoglobin, rbc counts and renal *Epo* mRNA levels relative to 18S for control (Co), *Foxd1*^{Cre/+} *Phd1*^{fllox/fllox} (*Phd1*^{-/-}), *Foxd1*^{Cre/+} *Phd3*^{fllox/fllox} (*Phd3*^{-/-}) and *Foxd1*^{Cre/+} *Phd1*^{fllox/fllox} *Phd3*^{fllox/fllox} (*Phd1*^{-/-}*Phd3*^{-/-}) mutant mice (n=3-5). Data are represented as mean ± SEM; 2-tailed Student's *t*-test. Significant differences were not found between groups.



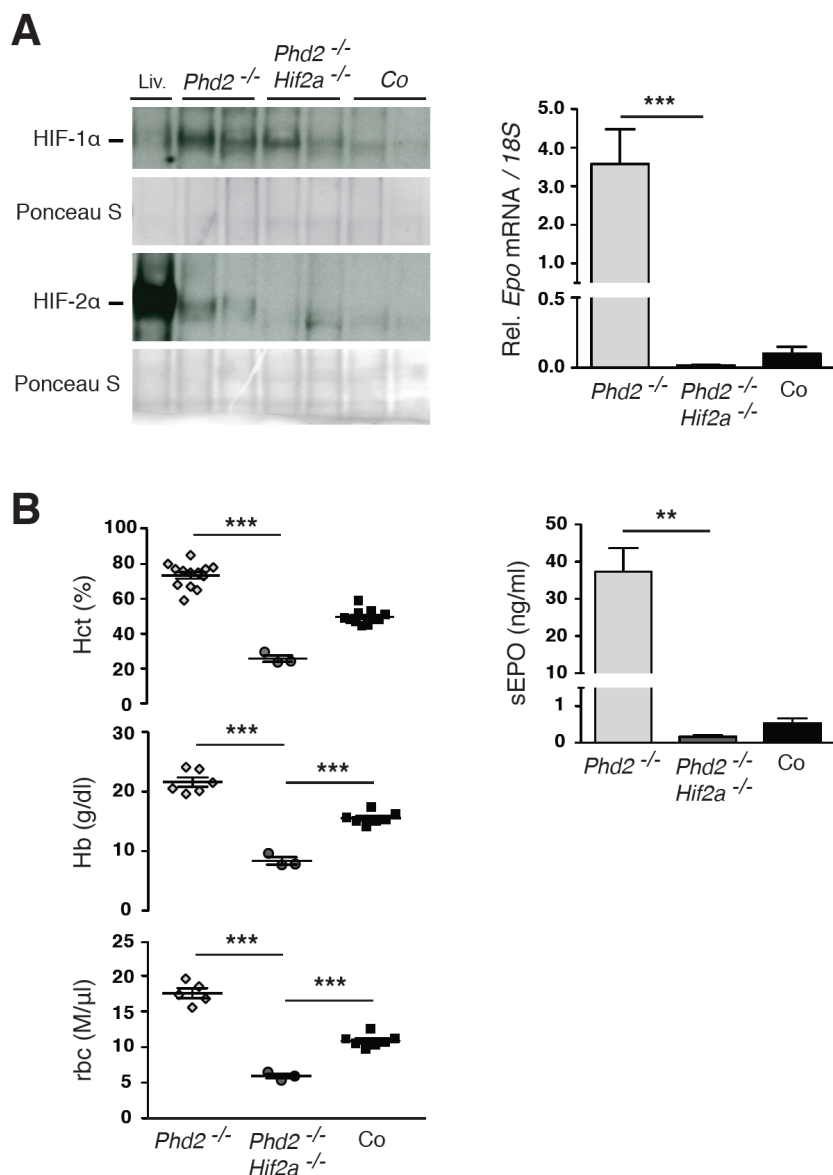
Supplemental Figure 4. HIF-2α and not HIF-1α is stabilized in *Foxd1-Phd2*^{-/-} kidneys. (A-H) Representative images of IHC stains for HIF-1α and HIF-2α in formalin-fixed, paraffin-embedded kidney tissue sections from *Cre*⁻ control and *Foxd1*^{Cre/+} *Phd2*^{flox/flox} mutant mice (*Phd2*^{-/-}). (A, E) *Cre*⁻ control; (B, F) negative control without primary antibody; (C) HIF-1α staining in a *Phd2*^{-/-} kidney; (D) HIF-1α staining in kidney from *Phd2*^{-/-} mouse treated with HIF prolyl-4-hydroxylase inhibitor GSK1002083A (PHI); (G) HIF-2α staining in a *Phd2*^{-/-} kidney; (H) HIF-2α staining in kidney from *Phd2*^{-/-} mouse treated with PHI. In PHI-treated mice nuclear HIF-1α staining was observed in renal tubular epithelial cells (black arrows) and in glomerular cells (red arrows), but not in interstitial cells. Nuclear HIF-2α staining was found in *Phd2*^{-/-} kidneys and was localized to interstitial (black arrows) and glomerular cells (red arrows). Our IHC data indicate that *Foxd1-Cre*-mediated *Phd2* inactivation resulted in nuclear HIF-2α accumulation but not HIF-1α stabilization in interstitial cells. PHI treatment increased the number of HIF-2α⁺ cells in *Phd2*^{-/-} kidneys. (I, J) HIF-1α and HIF-2α detected by immunoblot in whole kidney nuclear extracts from *Cre*⁻ control (Co) and *Foxd1*^{Cre/+} *Phd2*^{flox/flox} mice (*Phd2*^{-/-}). Ponceau S staining was used to assess for equal protein loading.



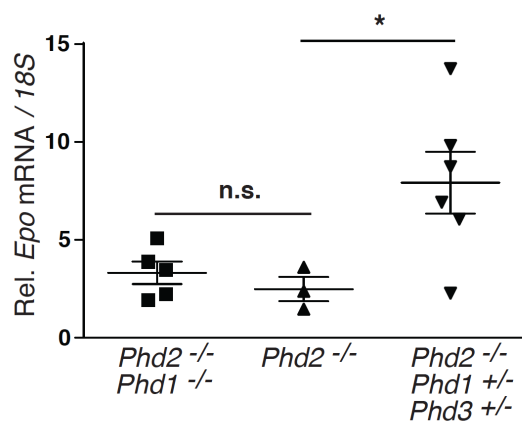
Supplemental Figure 5. *Epo* expression in *Phd2^{-/-}* kidneys is restricted to peritubular interstitial cells and does not associate with *Acta2* expression. (A) Representative images of multiplex ISH studies using formalin-fixed, paraffin-embedded kidney tissue sections from *Foxd1^{Cre/+} Phd2^{flox/flox} ROSA26-ACTB-tdTomato,-EGFP* and *Foxd1^{Cre/+} Phd2^{flox/flox}* mice. White arrows depict *Epo* transcripts (red signal). *Epo*⁺ cells in *Foxd1^{Cre/+} Phd2^{flox/flox}* kidneys did not express *EGFP* due to the absence of the double fluorescent Cre-reporter allele. Red arrowhead depicts *EGFP* transcripts in FOXD1 stroma-derived cells in vessel wall; white arrowhead depicts *EGFP* transcripts in glomerular cells with a history of FOXD1 expression. (B) *Epo* mRNA levels relative to *18S* detected by real time PCR in magnetic beads-enriched PDGFRB⁺ and PDGFRB⁻ cell fractions from control *Cre⁻* (Co) or *Foxd1^{Cre/+} Phd2^{flox/flox} (Phd2^{-/-})* kidneys (n=3). Graph bars represent mean ± SEM. (C) Multiplex ISH studies using formalin-fixed, paraffin-embedded kidney tissue sections from phlebotomized *Foxd1^{Cre/+} ROSA26-ACTB-tdTomato,-EGFP* mice. *Epo* transcripts were detected by red signals in peritubular interstitial cells only (white arrows). *EGFP* transcripts were detected by green signals, *Acta2* transcripts by blue signals. # denotes arterial vessel; asterisks denote glomeruli.



Supplemental Figure 6. *Ng2-Cre* targeted interstitial cells participate in renal EPO responses and are insensitive to *Phd2* inactivation. *Ng2-Cre Phd2*^{fllox/fllox} mice were characterized by normal erythropoiesis and did not display any obvious macroscopic or microscopic renal pathology. (A) Shown are values for hematocrit (Hct), hemoglobin (Hb), and rbc counts from individual *Cre*⁻ control (Co) and *Ng2-Cre Phd2*^{fllox/fllox} (*Phd2*^{-/-}) mutant mice (n=6 and 8 each). (B) Renal *Epo* mRNA levels from control and *Ng2-Cre Phd2*^{fllox/fllox} mutant mice at baseline and following intraperitoneal injection with recombinant human (rh) EPO (n=3-8). Renal *Epo* transcript levels are suppressed in rhEPO-injected *Ng2-Cre Phd2*^{fllox/fllox} mice indicating normal physiologic behavior of *Ng2-Cre* targeted renal interstitial cells. (C) Cells targeted by *Ng2-Cre* respond to hypoxia with *Epo*-induction. Shown is the percentage of NG2 *Epo*⁺ cells in *Ng2-Cre ROSA26-ACTBtdTomato,-EGFP* (Co) at baseline and following phlebotomy, and in *Ng2-Cre Phd2*^{fllox/fllox} *ROSA26-ACTBtdTomato,-EGFP* (*Phd2*^{-/-}) at baseline. The data indicate that NG2 renal interstitial cells are able to participate in the renal EPO response to hypoxia. At baseline less than 10% of *EGFP*⁺ cells expressed *Epo*, while a large proportion of *Ng2-Cre* targeted *EGFP*⁺ cells responded to hypoxia with the induction of *Epo*. Data are represented as mean \pm SEM; 2-way ANOVA (B), 1-way ANOVA (C); **P* < 0.05, ***P* < 0.01, when compared to control group.

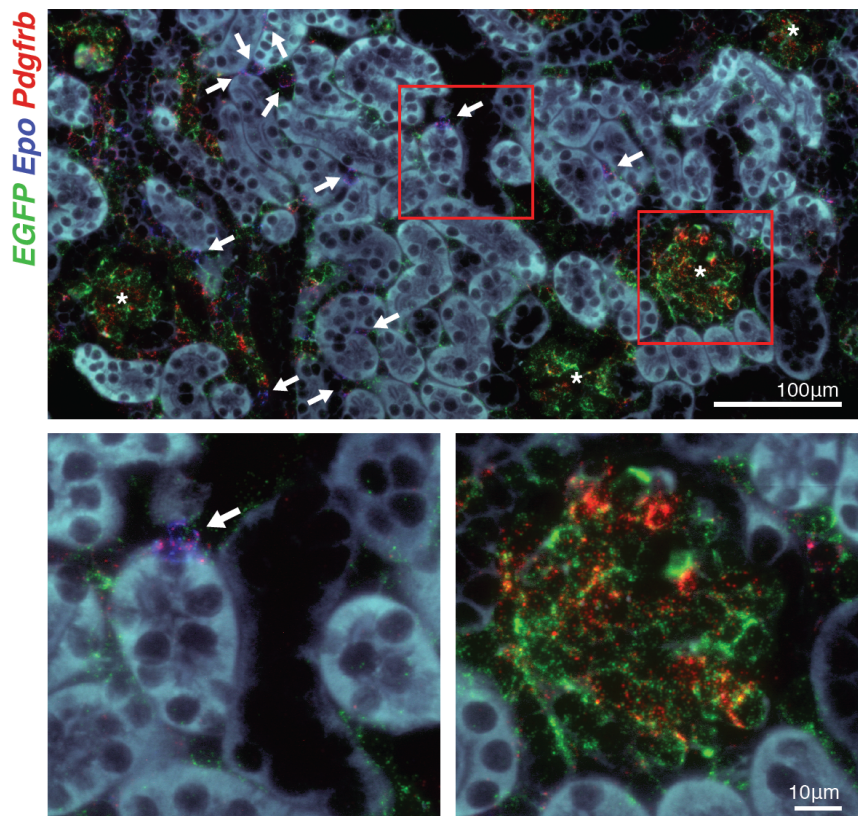


Supplemental Figure 7. *Epo* induction in *Phd2*^{-/-} kidneys is HIF-2-dependent. Results from conditional gene targeting studies using the *P3Pro-Cre* transgenic line (Kapitsinou et al., *Blood*. 2010;116(16):3039-3048) to inactivate *Phd2* and *Hif2a*. This transgenic line was generated by pronuclear injection; Cre-recombinase is under the control of the *Pax3* promoter. (A) Left panel: HIF-1 α and HIF-2 α detected by immunoblot in whole kidney nuclear extracts isolated from *P3Pro-Cre Phd2*^{flox/flox} (*Phd2*^{-/-}), *P3Pro-Cre Phd2*^{flox/flox} *Hif2a*^{flox/flox} (*Phd2*^{-/-} *Hif2a*^{-/-}) and *Cre*⁻ control (Co) mice. Whole liver nuclear extracts (Liv.) from mice with global *Vhl* gene deletion, which express high levels of HIF-2 α , served as positive control (Liu et al., *J Clin Invest*. 2012;122(12):4635-4644). Ponceau S staining was used to assess for equal protein loading. Right panel: *Epo* mRNA levels relative to 18S (n=3-7). (B) Hematocrit (Hct), hemoglobin (Hb), rbc counts and serum EPO (sEPO) levels in *P3Pro-Cre Phd2*^{flox/flox}, *P3Pro-Cre Phd2*^{flox/flox} *Hif2a*^{flox/flox} and *Cre*⁻ control mice (n=3-13). Data are represented as mean \pm SEM; 1-way ANOVA with post hoc Tukey's test; ***P* < 0.01 and ****P* < 0.001.



Supplemental Figure 8. Inactivation of *Phd1* does not affect renal EPO production in *Phd2*^{-/-} kidneys.

Shown are renal *Epo* mRNA levels relative to *18S* in total kidney homogenates isolated from *Foxd1*^{Cre/+} *Phd1*^{flox/flox} *Phd2*^{flox/flox} (*Phd1*^{-/-} *Phd2*^{-/-}), *Foxd1*^{Cre/+} *Phd2*^{flox/flox} (*Phd2*^{-/-}) and *Foxd1*^{Cre/+} *Phd1*^{+flox} *Phd2*^{flox/flox} *Phd3*^{+flox} (*Phd1*^{+/-} *Phd2*^{-/-} *Phd3*^{+/-}) mutant mice (n=5, 3 and 6 respectively). Data are represented as mean ± SEM; 1-way ANOVA with post hoc Tukey's test; **P* < 0.05; n.s., statistically not significant.



Supplemental Figure 9. Efficient detection of *Pdgfrb* in *Epo*-expressing cells in kidneys from *Pdgfrb-Cre Phd2^{flox/flox}* mutants. Representative images of multiplex ISH studies using formalin-fixed, paraffin-embedded kidney tissue sections from *Pdgfrb-Cre Phd2^{flox/flox} ROSA26-ACTB-tdTomato,-EGFP* mice. White arrows depict *Epo*⁺ cells that express *Pdgfrb* transcripts. *Epo* transcripts were detected by blue signals in peritubular interstitial cells only (white arrows), *EGFP* transcripts were detected by green signals and *Pdgfrb* transcripts by red signals. $93.2 \pm 3.5\%$ of *Epo*⁺ cells were found to express *Pdgfrb* transcripts indicating very good sensitivity of the *Pdgfrb* probe (n=3). Asterisks denote glomeruli.